ResearchGate

See discussions, stats, and author profiles for this publication at: https://www.researchgate.net/publication/30399830

Structure and Charge Distribution in Poly(styrenesulfonate) Ion Exchange Resins

ARTICLE *in* MACROMOLECULES · MARCH 1996

Impact Factor: 5.8 · DOI: 10.1021/ma951571s · Source: OAI

CITATIONS
9

READS
18

4 AUTHORS, INCLUDING:

Johan R C van der Maarel

108 PUBLICATIONS **1,718** CITATIONS

SEE PROFILE

Maxim E Kuil

Leiden University

42 PUBLICATIONS **694** CITATIONS

SEE PROFILE

Available from: Johan R C van der Maarel
Retrieved on: 26 January 2016

Structure and Charge Distribution in Poly(styrenesulfonate) Ion Exchange Resins

J. R. C. van der Maarel,*,† W. Jesse,† M. E. Kuil,† and A. Lapp‡

Leiden Institute of Chemistry, Gorlaeus Laboratories, Leiden University, P.O. Box 9502, 2300 RA Leiden, The Netherlands, and Laboratoire Léon Brillouin, Laboratoire Commun CEA-CNRS, C.E. Saclay, 91191 Gif sur Yvette, France

Received October 24, 1995; Revised Manuscript Received December 18, 1995[⊗]

ABSTRACT: Poly(styrenesulfonate) ion exchange resins were investigated with small angle neutron scattering. The polymer, polymer counterion, and counterion partial structure functions and charge structure function were obtained with contrast matching in water. In the reciprocal space interval $q < 1$ nm^{-1}, *all* partial structure functions display an upturn. This is attributed to different swelling of regions with differences in cross-link concentration, resulting in similar long range static heterogeneity in polymer and small ion density. The charge structure function was found to satisfy the sum rules and demonstrates the strong suppression of large scale temporal fluctuations. At larger wave vectors, the structure functions reflect the distribution of counterions with respect to the polymer charges. An effective charge screening length is obtained, and its value agrees with a strong association of the ionic species.

Introduction

Strong polyelectrolytes dissociate into highly charged polyions and their oppositely charged counterions. The spatial distribution of charges is related to the Coulomb interaction and possibly to relatively short ranged hydration effects. The counterions accumulate about the charged polymer with a reduction in their mobility. In previous work, both synthetic linear poly(styrenesulfonate) (PSS) and rodlike DNA fragments were investigated by using small angle neutron scattering with contrast matching in the water.[1−3] A complete picture of the solution structure was given by the set of spatial Fourier transforms of the polymer, polymer counterion, and counterion density correlation functions (partial structure functions). The results agree with a radial counterion distribution profile calculated by using the (modified) Poisson−Boltzmann equation.[4]

In the present paper, the work on synthetic linear polyelectrolytes has been extended to PSS ion exchange resins. These resins have found widespread technological (e.g., waste water treatment) and medical applications because of their ability to separate ions or molecules on the basis of their net charge. The functional SO_3^- groups are attached to a chemically cross-linked polystyrene matrix and counterions are reversibly adsorbed by electrostatic forces. The relative selectivity of various counterions indicates the importance of short range correlations between the cation and the polymer network. The main goal of the present research is the spatial distribution of polymer and counterion charges, which may provide some insight in the ion binding phenomenon.

The scattering units are tetramethylammonium (TMA^+) counterions, sulfonated styrene (SS^-) repeat units, and divinylbenzene (DVB) cross-linking units. The network might contain some styrene (S) monomers without a functional group. The latter units are present due to incomplete sulfonation of resins with a high degree of cross-linking. With 4 different scattering units, a full description of the structure requires 10 partial structure functions. In principle, these structure functions can be unraveled by measuring the SANS intensity of at least 10 samples with different contrast parameters. The abundant scattering units are the charge carriers TMA^+ and SS^-. For resins with a relatively low degree of cross-linking, the scattering contributions of cross-linking units and styrene monomers without a functional group can be neglected. The spatial distribution of the positive and negative charge carriers is described by three partial structure functions, which are obtained by measuring the SANS intensity of four chemically identical samples with different contrast with respect to water.

The mutual fluctuations of the positive and negative charges are most conveniently described by the charge structure function, i.e., the spatial Fourier transform of the charge density pair correlation function.[5] For the present resins, this function could be obtained in a single experiment with zero average collision amplitude contrast of the charge carriers.[6] The charge structure function should satisfy certain sum rules. In the long wavelength limit (i.e., for vanishing values of momentum transfer), this function goes to zero because of macroscopic electroneutrality. The second moment of the charge density pair correlation can be derived from the behavior at small values of momentum transfer ($q < \kappa$).[7] The second moment can be interpreted as an effective screening length κ^{-1} and provides information about the spatial distribution of the counterions with respect to the polymer matrix.

SANS of weakly charged polyelectrolyte gels shows a small angle upturn and a peak at higher values of momentum transfer.[8] The small angle upturn has been attributed to a static spatial heterogeneity in cross-link density, whereas the peak was assigned to temporal fluctuations in polymer density on a shorter distance scale. The intensities were not resolved into partial structure functions, so that no information about the counterion structure was derived. For PSS ion exchange resins, the existence of at least two characteristic length scales has been inferred from counterion quadrupolar relaxation and pulsed field gradient diffusion NMR.[9] The smallest length scale was shown to correspond to the intersegment distance, whereas the largest one reflects inhomogeneities in cross-link concentration. As in the case of weak polyelectrolyte gels,

* Author to whom correspondence should be addressed.
† Leiden University.
‡ Laboratoire Léon Brillouin.
[⊗] Abstract published in *Advance ACS Abstracts,* February 15, 1996.

0024-9297/96/2229-2039$12.00/0 © 1996 American Chemical Society

fluctuations at wave vectors corresponding to the inverse of these characteristic length scales will manifest themselves in the scattering behavior. The relative importance of spatial vs temporal fluctuations can be assessed on the basis of the full set of structure functions. In particular, it will be shown that there are no charge fluctuations associated with the long range static heterogeneities.

Theory

The general form of the coherent part of the solvent-subtracted SANS intensity reads

$$I(q) = \sum_{\alpha,\beta}[C_\alpha \bar{b}_\alpha{}^2 S_{\alpha\alpha} + 2\sqrt{C_\alpha C_\beta}\bar{b}_\alpha \bar{b}_\beta S_{\alpha\beta} + C_\beta \bar{b}_\beta{}^2 S_{\beta\beta}] \quad (1)$$

where $S_{\alpha\beta}$ is a partial structure function related to the scattering units α and β, with concentrations C_α and C_β and scattering length contrasts $\bar{b}_\alpha$ and $\bar{b}_\beta$, respectively. The partial structure function is the spatial Fourier transform of the pair correlation function $g_{\alpha\beta}(\bar{r})$ of the local concentration of species α and β:

$$S_{\alpha\beta}(q) = \delta_{\alpha\beta} + \sqrt{C_\alpha C_\beta}\int \mathrm{d}\bar{r}\ \mathrm{e}^{i\bar{q}\cdot\bar{r}}[g_{\alpha\beta}(\bar{r}) - 1] \quad (2)$$

For a H_2O/D_2O solvent mixture, the scattering length contrast is given by

$$\bar{b}_\alpha = b_\alpha - b_s \bar{\nu}_\alpha/\bar{\nu}_s \quad \text{with} \quad b_s = X b_{D_2O} + (1 - X) b_{H_2O} \quad (3)$$

where X denotes the D_2O mole fraction. The scattering lengths of the dispersed particle α and solvent s are denoted by b_α and b_s, respectively. The corresponding partial molal volumes are given by $\bar{\nu}_\alpha$ and $\bar{\nu}_s$.

In the ion exchange resin, the scattering units are TMA^+, SS^-, cross-linking units, and possibly monomers without a functional group. As a first approximation the latter two contributions are neglected. This assumption is reasonable for resins with a relatively low degree of cross-linking and nearly complete sulfonation levels. The abundant scattering units are the charge carriers TMA^+ and SS^- with equal concentrations $C_{TMA} = C_{SS} = C$. The charge system is described by the counterion TMA^+, polymer SS^-, and counterion polymer cross partial structure functions. These functions are denoted by S_{CC}, S_{PP}, and S_{PC}, respectively.

An interesting situation occurs when the collision amplitude contrasts of the counterion and sulfonated styrene monomer have the same absolute values, but opposite signs. Under this condition (zero average contrast), the intensity is directly proportional to the charge structure function:

$$S_{ZZ}(q) = S_{PP}(q) - 2S_{PC}(q) + S_{CC}(q) \quad (4)$$

which is the spatial Fourier transform of the charge pair correlation function

$$S_{ZZ}(q) = 2 + C\int \mathrm{d}\bar{r}\ \mathrm{e}^{i\bar{q}\cdot\bar{r}} g_{ZZ}(\bar{r}) \quad (5)$$

with

$$g_{ZZ}(\bar{r}) = g_{CC}(\bar{r}) + g_{PP}(\bar{r}) - 2g_{PC}(\bar{r}) \quad (6)$$

The charge structure function satisfies the Stillinger–Lovett sum rules.[7] In the long wavelength limit ($q \to 0$), electroneutrality requires that the charge structure tend to zero. By expanding eq 5 up to the second power of q, one obtains the limiting law

$$S_{ZZ}(q) = 2q^2/\kappa^2 \quad (q < \kappa) \quad (7)$$

The effective screening length κ^{-1} is the second moment of the charge density pair correlation function and takes the form

$$2/\kappa^2 = -(C/2)\int \mathrm{d}\bar{r}\ (\hat{q}\cdot\bar{r})^2 g_{ZZ}(\bar{r}), \quad \hat{q} = \bar{q}/|q| \quad (8)$$

The screening length is necessarily positive, because the structure function eq 7 is a square amplitude.

Experimental Section

Analytical grade poly(styrenesulfonic acid) cation exchange resin type AG 50W was obtained from Bio-Rad Laboratories. The polymer network exists of polystyrene chain segments that are covalently cross-linked with 2, 4, 8, 12, and 16% DVB (denoted by X-2, etc.). The average number of repeat units (degree of polymerization) of the chain segments is approximately 30, 15, 7, 5, and 3, respectively.[9] The functional sulfonate groups (SO_3H) are attached to the styrene repeat units. The resins were first brought into the pure acid form by flushing with 2 M HCl and deionized water (filtered by Millipore Co. water purification system) until the conductivity of the elute did not exceed $1 \times 10^{-6}\ \Omega^{-1}\ \mathrm{cm}^{-1}$. The hydrogen counterions were subsequently exchanged by TMA^+ ions. For this purpose, the materials were flushed with 0.25 M TMAOH and left overnight. Excess alkali was removed by rinsing with water. Before sample preparation, the resins were dried at 313 K under reduced pressure over P_2O_5. The water content of the dried materials was determined by IR spectroscopy and found to be on the order of 2%.

Samples were prepared by swelling the dried resin beads in H_2O/D_2O isotopic mixtures. Standard quartz sample containers with 0.2 (for D_2O-containing samples) or 0.1 cm path length were used. The resins were at the swelling equilibrium, the space between the beads was filled with solvent. The size of the swollen beads is on the order of 50−1000 μm, but decreases with increasing cross-linkage. It was checked that the swelling equilibrium did not depend on the isotopic composition of the solvent. Concentrations of cross-links (DVB), styrene monomers (S), and sulfonated styrene repeat units (SS) were determined by weight, taking into account the molar fraction of cross-links in the reaction mixture prior to polymerization and the degree of sulfonation. The degree of sulfonation was obtained by the titration of fully swollen and protonated resins.[9] The highly cross-linked X-12 and X-16 resins in particular are characterized by incomplete sulfonation levels. The results are collected in Table 1. The concentrations are average values over the whole irradiated sample volume (with 8 mm cross-section diaphragm); locally inside the beads the concentrations are higher. The X-2, X-4, and X-12 resins were swollen in four different solvents with D_2O mole fractions 0, 0.25, 0.43, and 0.99, respectively. The 8 and 16% cross-linkages were investigated in pure D_2O only. The scattering length contrasts of TMA and SS were calculated by using eq 3 and the parameters in Table 2. The results are collected in Table 3.

Neutron scattering experiments were performed by using two different small angle scattering instruments. The X-2, X-4, and X-12 resins were investigated by using the PAXY diffractometer, situated on the cold source of the high neutron flux reactor at the Laboratoire Léon Brillouin, CEN-Saclay, France. Two sets of data were collected in different experimental configurations. In the first configuration, a wavelength of 0.4 nm was selected, and the effective distance between the sample and the planar square multi detector was 1.03 m. This allows for a momentum transfer range of 0.8−5 nm^{-1}. The counting time per sample or solvent was approximately 4 h. In the other configuration, the detector was placed at a distance of 3.2 m from the sample, and a neutron wavelength of 0.8 nm was selected. Here, the momentum transfer ranged from 0.1 to 0.9 nm^{-1}, with a counting time of approximately 7 h/sample.

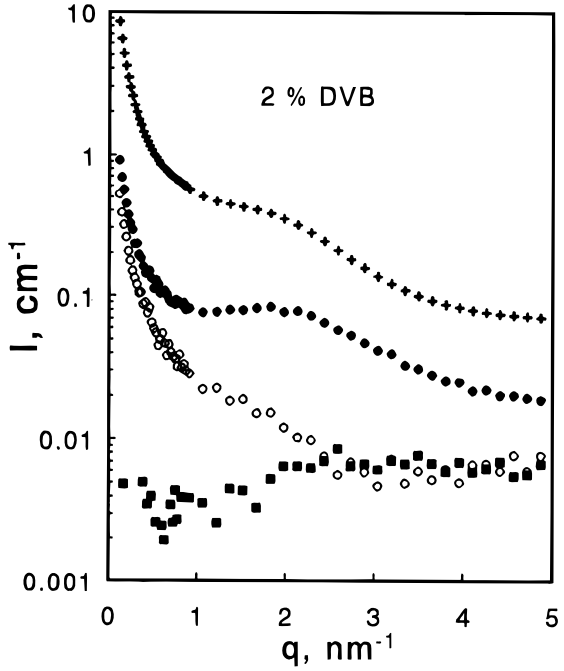

Figure 1. Experimental intensities for the X-2 TMAPSS ion exchange resin. The symbols refer to resins swollen in the solvents: +, 100% D_2O; ○, 43% D_2O; ■, 25% D_2O; ●, H_2O.

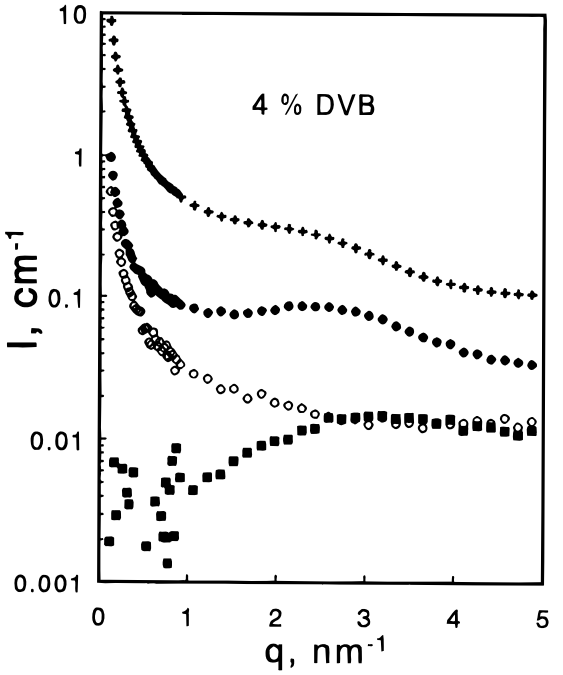

Figure 2. Same as in Figure 1, but for the X-4 resin.

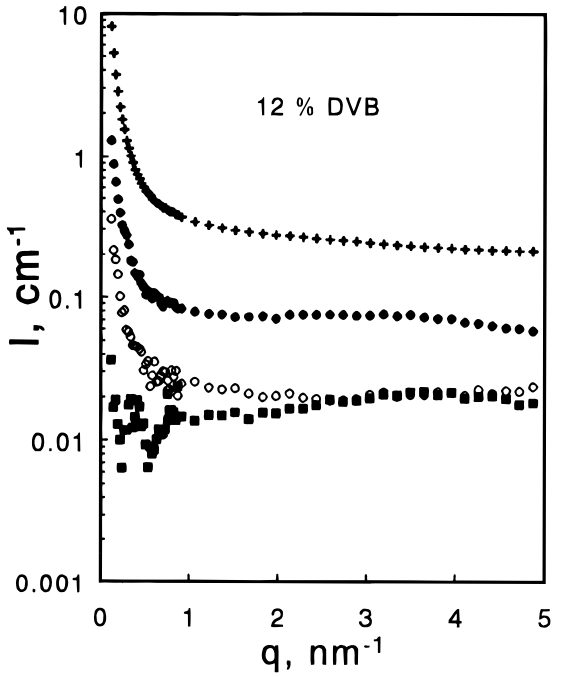

Figure 3. Same as in Figure 1, but for the X-12 resin.

All resins, but in D_2O only, were investigated using the LOQ small angle scattering instrument, situated on the pulsed spallation neutron source of the ISIS facility, Rutherford Appleton Laboratory, Didcot, UK. The incident wavelength was 0.2−1 nm at a pulse rate of 25 Hz. The scattered radiation was detected by using a two-dimensional detector that was 4.4 m from the sample position, allowing a momentum transfer range of 0.1−2 nm^{-1}. The counting time was approximately 4 h/sample.

Data correction allowed for sample transmission, detector efficiency, and, in the case of the spallation source data, the incident neutron spectrum shape. Absolute scattering intensities were obtained by reference to water and to the coherent scattering from a partially deuterated polystyrene sample for the PAXY and LOQ data, respectively. The scattering of the corresponding solvents was subtracted, and the data were corrected for the incoherent scattering of the polymer. It was observed that both instruments yield identical results for the same sample in the overlapping momentum transfer range. However, due to the adjustable sample to detector distance, the PAXY instrument allows for a more extended range of momentum transfer. The temperature was kept at 298 K.

Results and Discussion

For the X-2, X-4, and X-12 resins, the scattering length contrast was varried by adjusting the H_2O/D_2O solvent ratio. The scattered intensities vs momentum transfer are displayed in Figures 1−3, respectively. The intensities are strongly influenced by solvent composition. In pure H_2O, the TMA^+ counterion has a negligible scattering length contrast; the scattering is completely due to the polymer (see Table 3). The samples in D_2O of mole fraction 0.25 satisfy the zero average contrast condition, i.e., the TMA^+ and SS^- scattering length contrasts have the same absolute values, but opposite signs. The intensity is directly proportional to the charge structure function, provided that the scattering contributions of cross-links and/or units without a functional group can be neglected. In D_2O of mole fraction 0.43, the sulfonated styrene monomer has zero scattering length contrast, and the intensity is dominated by the counterion structure. The scattering of the samples in D_2O is the most intense due to the relatively large contrast length parameters. All resins in D_2O (including X-8 and X-16) were investigated by using the LOQ instrument as well. The corresponding intensities divided by concentration are displayed in Figure 4.

Most samples show an upturn in intensity at low values of momentum transfer $q < 1$ nm^{-1}, except those with zero average scattering length contrast (D_2O of mole fraction 0.25). Apart from the small angle upturn, the samples in pure H_2O and D_2O display a maximum in intensity at higher values of momentum transfer. The latter maximum is observed in solutions of linear polyelectrolytes as well and is related to temporal fluctuations in polymer and counterion concentration.[1−3] For the resins, the peak merges into the small angle upturn and takes the form of a shoulder. It shifts to higher values of momentum transfer with increasing

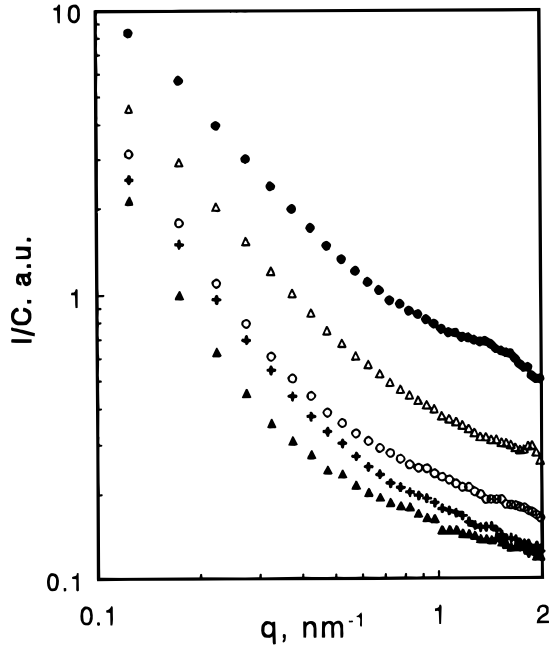

Figure 4. Experimental intensities divided by the concentration for TMAPSS ion exchange resins in D_2O. The symbols refer to the resins: ●, X-2; △, X-4; ○, X-8; +, X-12; ▲, X-16.

Table 1. Concentrations of TMAPSS Ion Exchange Resin

cross-linkage (%)	$C_{TMA} = C_{SS}$ (mol/L)	C_S (mol/L)	C_{DVB} (mol/L)	degree of sulfonation
2	0.65		0.01	1
4	1.19	0.02	0.04	0.98
8	1.72	0.02	0.08	0.99
12	2.00	0.25	0.25	0.89
16	1.80	0.34	0.38	0.84

Table 2. Partial Molal Volumes and Scattering Lengths

solute	$\bar{v}_i$ (cm^3/mol)	$\bar{b}_i$ (10^{-12} cm)
SS	114	4.72
TMA	84	11.6
H_2O	18	−0.168
D_2O	18	1.915

cross-link density. These features will be discussed further in the following, when the experimental intensities are decomposed into the partial structure functions.

The scattering contributions of cross-linking units and/or units without a functional group (styrene monomers) will be neglected. This approximation is reasonable for the X-2 and X-4 resins, which have a low concentration of DVB and nearly complete levels of sulfonation (see Table 1). As will be shown later, this conjecture breaks down for resins with a higher degree of cross-linking. The X-2, X-4, and X-12 data represent overdetermined sets from which the partial structure functions related to the charge carriers can be derived. The intensities of the samples in D_2O of mole fractions 0, 0.25, and 0.43 are directly proportional to the polymer, charge, and counterion structure function, respectively. The best solutions to the complete data set (including the sample in D_2O) were obtained by using QR factorization with the concentrations and scattering length densities given in Tables 1 and 3, respectively. The results of this least-squares procedure are displayed in Figures 5 and 6 for the low and high q regions, respectively. The charge structure function was obtained from the combination of the partial structure functions according to eq 4 and is displayed in Figure 7. It was verified that the derived partial structure

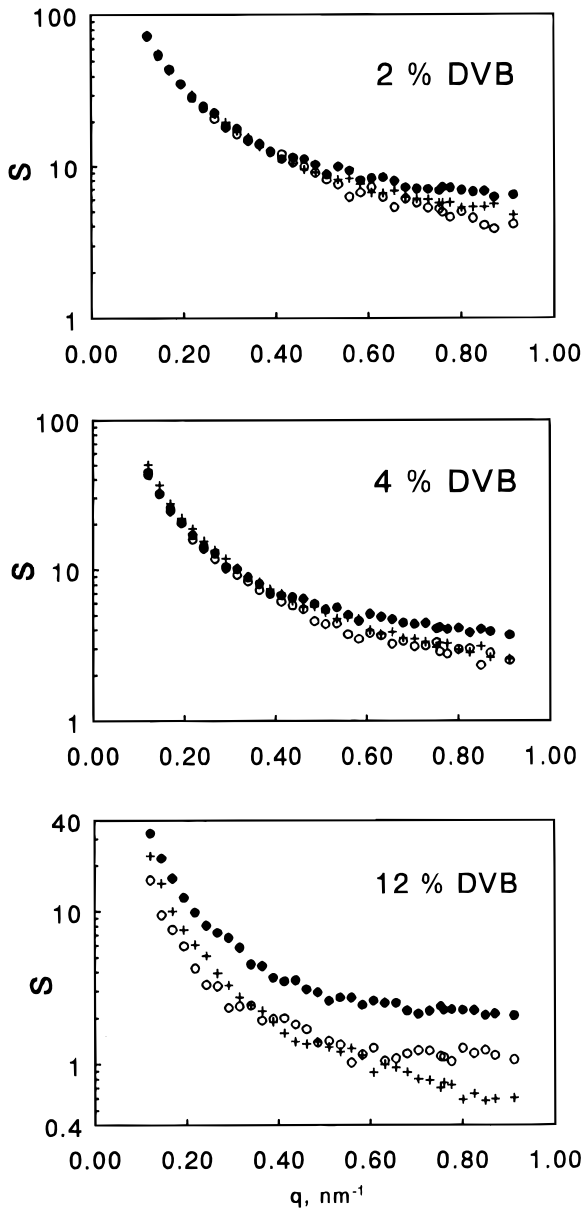

Figure 5. Partial structure functions in the low q range. From top to bottom: 2, 4, and 12% cross-linkages, respectively. The symbols refer to the polymer (●), polymer counterion (+), and counterion (○) partial structure functions.

Table 3. Scattering Length Contrast of TMA Counterions and Sulfonated Styrene Monomers

mole fraction of D_2O	$\bar{b}_{TMA}$ (10^{-12} cm)	$\bar{b}_{SS}$ (10^{-12} cm)
0	−0.1	5.8
0.25	−2.5	2.5
0.43	−4.3	0
0.99	−9.8	−7.4

functions are consistent with the experimental intensities within statistical error (data not shown).

All partial structure functions show a low q upturn and, at least for X-2 and X-4, take a common long wavelength ($q \to 0$) value. This is most clearly demonstrated by the charge structure function. In the long wavelength limit, the charge structure function should be zero in accordance with macroscopic electroneutrality. For the X-12 resin, the charge structure function does not take the correct limiting value. This is related to the neglect of the scattering contribution of the cross-linking units and/or styrene monomers (incomplete sulfonation).

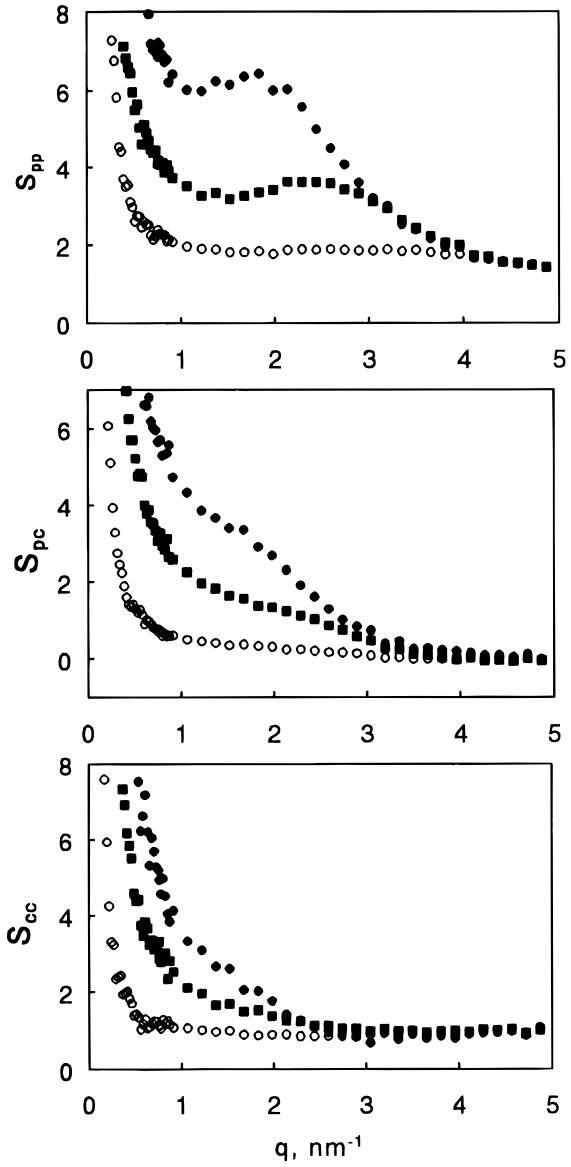

Figure 6. Partial structure functions in the high q range. From top to bottom: polymer, polymer counterion, and counterion partial structure functions. The symbols refer to cross-linkages: ●, X-2; ■, X-4; ○, X-12.

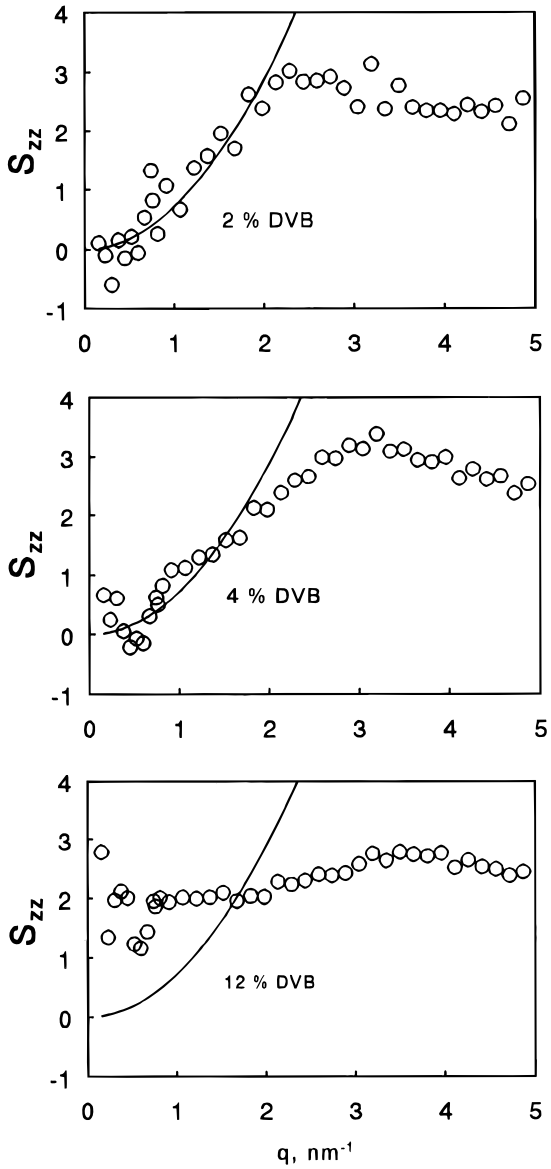

Figure 7. Charge structure functions for X-2, X-4, and X-12 from top to bottom, respectively. The solid line refers to the Stillinger−Lovett second moment law, with the charge screening length being equal to 0.6 nm. In the low q region the data are rebinned.

The present low q behavior of the partial structure functions is different from the situation in solutions of linear polyelectrolytes. In the latter solutions, the only contributions are fluctuations in polymer and counterion concentration. However, any large scale concentration fluctuations are suppressed by electrostatic interactions, resulting in a relatively high value of osmotic compressibility and, hence, a small thermodynamic limit of the structure functions.[10−12] An additional small angle upturn was observed for weakly charged polyelectrolyte gels as the swelling equilibrium is approached.[8] This effect was assigned to inhomogeneities in cross-link density. Regions with different cross-link density swell differently, causing a long range static heterogeneity in polymer concentration. The present highly charged PSS resins are at the swelling equilibrium. The low q behavior of the partial structure functions indicates a similar long range heterogeneity in polymer and counterion structure. The charge structure function shows that large scale temporal fluctuations are suppressed.

As was shown for the X-2, X-4, and X-12 resins, in the low q region the partial structure functions display a similar upturn. Accordingly, to investigate the dependence on the cross-linkage of the large scale heterogeneity, a decomposition of the experimental intensities into contributions of polymer and/or counterions is not necessary. Figure 4 displays a double-logarithmic plot of the intensity divided by polymer concentration for all resins in D_2O. No linearity over a sufficiently extended range of momentum transfer is observed. The small q limiting scattering exponent ranges from 1.3 for X-2 to 1.7 for the highly cross-linked X-16 resin. The data could not be interpreted with a Debye−Bueche law, representing scattering from heterogeneities with flat interfaces. However, the slight increase in the limiting scattering exponent signifies a growth in the heterogeneities with an increasing degree of cross-linking. The concurrent decrease in the long wavelength limit of the structure functions (Figure 5) indicates a smaller spatial variation in density.

For higher values of momentum transfer, the polymer, polymer counterion, and counterion partial structure functions diverge, and the polymer structure

function shows a polyelectrolyte shoulder at momentum transfer q_m. This shoulder owes its existence to interferences between different chain segments. With increasing cross-link concentration the resins are more dense, and these interferences become progressively more important on a shorter distance scale. Accordingly, the shoulder shifts to higher values of momentum transfer. Concurrently, it becomes less intense and almost disappears in the case of the relatively dense X-12 resin. The drop in intensity is due to the monotonously decreasing particle form function.

The divergence of the partial structure functions at higher values of momentum transfer reflects the shell-like clustering of counterions about the chain segments. In linear polyelectrolyte solutions, the structure functions were found to agree with calculations according to the cell model and a counterion profile away from the polymer axis.[1−4] For the present dense systems, this approach is bound to fail due to important intersegment interference effects at higher q values. A quantitative interpretation of the latter effects cannot be given, since this requires a complete description of the gel structure. However, information concerning charge ordering can be obtained from the charge structure function, in which the effects of longer ranged correlations in counterion and polymer density (such as static inhomogeneities) are seen to vanish.

The charge structure function reflects the counterion accumulation about a charged chain segment, which is expected to be rather insensitive to cross-link density. Indeed, as observed in Figure 7, the X-2 and X-4 resins have a similar charge structure. The X-12 resin shows a moderate low q upturn in the charge structure function as well, which is due to the scattering contribution of the cross-linking units and/or incomplete sulfonation. The neglect of the latter contributions is reasonable for resins with a cross-link percentage of less than, say, 8%. The charge structure displays a maximum for wave vectors corresponding to the inverse double-layer thickness. This maximum shifts to higher q values with increasing cross-link concentration. More precise information concerning charge screening can be obtained from the Stillinger−Lovett sum rules.[7] In the long wavelength limit, charge fluctuations are suppressed and macroscopic electroneutrality requires that the charge structure function tend to zero. As discussed before, this behavior is indeed observed for the X-2 and X-4 resins. The second moment law (eq 7), with a second moment of the charge density pair correlation function being equal to 0.6 nm, is also displayed in Figure 7. Again, for the X-2 and X-4 resins there is reasonable agreement. The screening length is on the order of the distance of closest approach of the counterion to the polymer chain and reflects the strong affinity of the counterions for the negative charges attached to the polymer matrix.

Conclusions

The presence of at least two different structural length scales was already inferred from counterion quadrupolar nuclear magnetic relaxation and diffusion studies.[9] The smallest length scale corresponds to the intersegment distance, whereas the largest one reflects inhomogeneities in cross-link density. The present neutron scattering results demonstrate that the fluctuations at wave vectors corresponding to the inverse of these length scales are fundamentally different.

All partial structure functions show a low q upturn. This behavior can be attributed to inhomogeneities in cross-link density. Regions that differ in cross-link density swell differently, resulting in identical long range static heterogeneity in polymer and counterion density. Large scale temporal fluctuations in polymer and counterion concentration are strongly suppressed due to the huge electrostatic energies involved. This is most clearly demonstrated by the charge structure function. The latter function satisfies the Stillinger−Lovett sum rules and tends to zero in the long wavelength limit. A more precise picture of the heterogeneities is difficult to extract from the present data, because existing relations, such as Porod's or Debye−Bueche's laws, were unable to reproduce the basic features. However, the results indicate a growth in the heterogeneities and a smaller spatial variation in density with increasing cross-link concentration. The heterogeneities extend over an increasingly larger number of cross-links, because the length of the chain segments between cross-links decreases from roughly 8 (X-2) to 1 (X-16) nm.[9] These observations might help to explain the differences in porosity and selectivity of the various resins.

The scattering behavior at higher values of momentum transfer is substantially different. Here, the partial structure functions diverge and reflect the shell-like clustering of counterions about the chain segments. The position of the shoulder is very sensitive to cross-link density, mainly because of differences in polymer concentration. Interferences between different polymer segments are very strong and preclude a complete quantitative interpretation of the partial structure functions. However, an effective charge screening length can be derived from the Stillinger−Lovett second moment law. This length takes the value 0.6 nm, irrespective the cross-link density. Unfortunately, this could be verified for the X-2 and X-4 resins only. For the X-12 resin, the scattering contributions of the cross-linking units and/or units without a functional group can no longer be neglected. The effective screening length is approximately the distance of closest approach of the counterion to the chain. This short distance and the absence of charge fluctuations at longer wavelengths show that the counterions are strongly associated with the polymer functional groups. This is also supported by high-resolution neutron diffraction on X-8 Li- and Ni-PSS resins, which agrees with a penetration of the polymer functional group into the primary hydration sheath of the counterions.[13]

For polystyrene-based ionomer membranes with low ion contents (less than 10−20%), scattering behavior similar to the present results has been observed.[14−16] Anomalous small angle X-ray scattering has shown that both the ionic peak and small angle upturn are related to the spatial distribution of the ionic groups. The upturn is usually interpreted as a result of multiplet formation, i.e., aggregates of tightly packed ion pairs dispersed in the polymer matrix. However, in the PSS resins, nearly every monomer carries a charge and multiplet formation is difficult to conceive.

Acknowledgment. We thank R. K. Heenan and S. M. King for their assistance during the LOQ experiment and for critical reading of the manuscript. The staff of the ISIS facility and Laboratoire Léon Brillouin are gratefully acknowledged for technical support. We thank R. H. Tromp for communication his diffraction results prior to publication. We are indebted to the Nederlandse Organisatie voor Wetenschappelijk Onderzoek (NWO) for financial support of the ISIS experi-

ment. The experiment at the Laboratoire Léon Brillouin was financially supported through the Large Installations Program of the European Community.

References and Notes

(1) van der Maarel, J. R. C.; Groot, L. C. A.; Mandel, M.; Jesse, W.; Jannink, G.; Rodriguez, V. *J. Phys. II Fr.* **1992**, *2*, 109.
(2) van der Maarel, J. R. C.; Groot, L. C. A.; Hollander, J. G.; Jesse, W.; Kuil, M. E.; Leyte, J. C.; Leyte-Zuiderweg, L. H.; Mandel, M.; Cotton, J.-P.; Jannink, G.; Lapp, A.; Farago, B. *Macromolecules* **1993**, *26*, 7295.
(3) Groot, L. C. A.; Kuil, M. E.; Leyte, J. C.; van der Maarel, J. R. C.; Cotton, J. P.; Jannink, G. *J. Phys. Chem.* **1994**, *98*, 10167.
(4) Bhuiyan, L. B.; Outhwaite, C. W.; van der Maarel, J. R. C. *Phys. A*, in press.
(5) Hansen, J.-P.; Mc Donald, I. R. *Theory of simple liquids*; Academic Press: New York, 1986.
(6) Jannink, G.; van der Maarel, J. R. C. *Biophys. Chem.* **1991**, *41*, 15.
(7) Stillinger, J.; Lovett, R. *J. Chem. Phys.* **1968**, *49*, 1991.
(8) Schosseler, F.; Skouri, R.; Munch, J. P.; Candau, S. J. *J. Phys. II Fr.* **1994**, *4*, 1221.
(9) Tromp, R. H.; van der Maarel, J. R. C.; de Bleijser, J.; Leyte, J. C. *Biophys. Chem.* **1991**, *41*, 81.
(10) Mandel, M. *Encyclopedia of Polymer science and engineering*, 2nd ed.; John Wiley and Sons, Inc.: New York, 1988; Vol. 11, p 739.
(11) In refs 1−3, this behavior has indeed been observed for linear TMAPSS or TMADNA samples in pure H_2O, but for solutions containing D_2O the intensity increases with decreasing q at very low q values ($q < 0.2$ nm^{-1}). This effect is more or less proportional to the D_2O mole fraction and does not vanish under the zero average contrast conditions. An explanation has not been offered, but the present results indicate that it likely is not due to any spatial inhomogeneities in polymer structure or to an instrumental artifact.
(12) Barrat, J.-L.; Joanny, J.-F.; Pincus, P. *J. Phys. II Fr.* **1992**, *2*, 1531.
(13) Tromp, R. H.; Neilson, G. W. *J. Phys. Chem.*, in press.
(14) Jiang, M.; Gronowski, A. A.; Yeager, H. L.; Wu, G.; Kim, J.-S.; Eisenberg, A. *Macromolecules* **1994**, *27*, 6541.
(15) Samuel Ding, Y.; Hubbard, S. R.; Hodgson, K. O.; Register, R. A.; Cooper, S. L. *Macromolecules* **1988**, *21*, 1698.
(16) Moore, R. B.; Gauthier, M.; Williams, C. E.; Eisenberg, A. *Macromolecules* **1992**, *25*, 5769.

MA951571S